Analysis of Steel-Concrete Composite Buildings for Blast Induced Progressive Collapse

S Jeyarajan[1,*], J Y Richard Liew[1,2] and C G Koh[1,2]
[1]Department of Civil and Environmental Engineering, National University of Singapore, 1 Engineering Drive 2, Singapore 117576
[2]College of Civil Engineering, Nanjing Tech University, China

Received on 8 August 2014; Accepted 23 April 2015

ABSTRACT
This paper investigates the progressive collapse behaviour of steel concrete composite buildings subject to ground blast explosion using nonlinear dynamic analysis and conventional alternate path approach. The alternate path approach, which is a threat independent methodology, is commonly used as a design guide for minimising the potential for progressive collapse. This method may not be always conservative in assessing the robustness of the structure, especially for building subject to heavy blast loads and thus nonlinear analysis is often needed to investigate the building response under such extreme load. In the present paper, composite slab model based on equivalent area approach and composite joint model based on Eurocode's component method are proposed for nonlinear analysis of building framework. The analysis results show that a heavy blast load may wipe out a series of columns/beams at once instead of a single one. High blast pressure may also induce large lateral drift and lead to significant damage to structural elements spreading over several storeys of the building. Generally, such extensive damage cannot be captured using the alternate path approach. The present investigation recommends that nonlinear analysis should be performed in order to capture the true behaviour of such buildings subject to extreme blast loads.

Key words: alternate path approach, blast load, collapse analysis, composite building, progressive collapse, robustness

1. INTRODUCTION

Research on the progressive collapse of building structures has been initiated with the partial collapse of Ronan Point apartment, UK, due to a domestic gas explosion. It has been intensified after several recent high profile collapses of multi-storey buildings [1–6]. Some of the major progressive collapse incidents that have occurred in the past have been: (i) 9-storey

*Corresponding author. E-mail address: Dr Jeyarajan Selvarajah eng.rajan@gmail.com

reinforced concrete Murrah Federal office building at Oklahoma City collapse due to a truck-bomb attack, and (ii) World Trade Centre twin towers and World Trade Centre 7 collapse due to terrorist attack. In this respect, the Alternate Path (AP) approach, which is a threat independent methodology, is commonly used as a design guide for minimising the potential for progressive collapse [7]. Nevertheless, the effectiveness of this method is still questionable for abnormal loads, because a single member is generally removed, although the method does not exclude the possibility of removing more than one member. This assumption may lead to inaccurate prediction of the building response, especially under heavy blast loads and thus nonlinear analysis is performed to investigate the building response under extreme load. The nonlinear analysis is performed herein using two-stage analysis, namely blast analysis and collapse analysis. The US guideline TM-5-1300 [8] shall be adopted for the blast analysis to calculate the blast pressure-time history on each structural element due to blast. The blast analysis is performed to identify the damaged elements in the building frame for subsequent collapse analysis. The structural element is considered as damaged/incapable, if the demand on a structural element exceeds its resistance or prescribed limits, such as rotation capacity or ductility limit given in design guidelines (e.g. GSA [7] are exceeded. The structural element damage criteria may be governed by the respective resistance to axial force, bending moment, shear force, or a combination of these, or may be due to limit of deflection or rotation at accident limit states. Based on the blast analysis result, damaged elements are removed from the building for the subsequent collapse analysis, which is performed as second stage analysis to predict the building response under extreme load. Many researchers have investigated the blast effects on steel and concrete buildings but very little research work has been reported for steel-concrete composite buildings and there is a need to investigate the robustness of composite frames under blast loading. EN1991-1-7 [9] highlights to perform systematic risk assessment for high consequences of failure. Therefore nonlinear analysis by taking care of probable extreme loading scenarios could be preferred for the robustness analysis of building structures.

Shi et al. [10] studied a three-storey two-span reinforced concrete (RC) frame for possible progressive collapse under a blast. Blast analysis results were compared with the results from an alternative path approach. The authors reported that the blast analysis can predict more accurately the structural progressive collapse process than the alternate path approach. Ngo et al. [11] presented a comprehensive overview of the effects of explosion on structures. An explanation of the nature of explosions and the mechanism of blast waves in free air was provided. The authors also introduced different methods to estimate blast loads and structural response. Draganic and Sigmund [12] described the process of determining the blast load on structures and investigated a reinforced concrete structure subject to blast load. Raparla and Kumar [13] studied the linear response of different RC bare frames subject to the blast of different charge weights. They found that the increase in structural response (e.g. displacement) was not linearly related to the charge weight and the displacement response was low for heavy structures compared to lighter structures.

Serdar et. al. [14] investigated the dynamic response of reinforced concrete (RC) columns subjected to axial and blast-induced transverse loads. The study concluded that the level of axial compressive load has significant influence on the buckling resistance of RC columns subjected to transverse blast-induced loads. Many researchers investigated the RC building frames' components response subject to blast load [15, 16, 17 and 25]. Damage level of RC beams under different blast loading was experimentally investigated by Zhang et al. [18], and the tests showed that the concrete spallation area on the RC beams increased with the decrease of the scaled distance of the explosion. The concrete beams were prone to be damaged in flexure mode with concrete crushed on the front face, concrete spallation on the back surface and concrete flake off on the side surface. Said and Bilal [19] explored the use of fiber reinforced plastic cable to strengthen the continuous concrete beam to mitigate progressive collapse due to the loss of an interior column.

Li et al. [20, 21] proposed a drift-controlled design method to predict the response of a reinforced concrete frame using equivalent static force from a blast loading. The equivalent static force was obtained by keeping the maximum inter-storey drift ratios same as those from blast loading. Blast and progressive collapse analyses were carried out by Tarek et al. [22] to establish the vulnerability of a typical multi-storey reinforced concrete building subjected to accidental load. The blast and residual resistances of a reinforced concrete building was investigated by a two-stage analysis approach by Jayasooriya et al. [23]. The first stage involved linear time history analysis, which was carried out to verify the global response of a frame and its ability to restore global frame stability. An explicit analysis accounting for strain rate effects of the reinforced concrete elements was carried out in second stage to investigate the non-linear response of vulnerable elements identified in the first stage. The damage mechanisms and the extent of damage were studied using principal stress and plastic strain behaviour. Using the stress and strain plots, residual capacities of key elements were estimated. Luccioni et al. [24] carried out nonlinear analysis on a damaged reinforced concrete building under a blast load. Elsanadedy et al. [26] performed a progressive collapse analysis of a multi-storey steel building subject to blast loads. The building was vulnerable to progressive collapse for a blast load of 500 kg and they concluded that a charge weight of 500 kg could cause progressive collapse of the building.

Fu [47] numerically investigated the robustness of a steel tall building under a package bomb blast of 15 kg, which was detonated at the 12^{th} level. Comparison between the blast analysis and alternate path approach were reported. The author concluded that (1) the conventional alternate path approach is conservative compared to the blast analysis due to dissipation of blast pressure upward and downward on the slab; (2) the alternate path approach ignores the huge shear force on the column due to the blast pressure; (3) the ductility and shear resistance of the column is important to avoid progressive collapse and (4) small scale blasts such as a package bomb could hardly trigger the progressive collapse of building.

Although progressive collapse analysis procedure is similar for steel and reinforced concrete (RC) building as per GSA guideline, a RC building behaves differently under a blast load compared to a steel building in terms of joint and material behaviour, frame response and floor slab reinforcement configurations. Column-to-beam and beam-to-beam connections in a RC building are rigid, whereas connection of a steel-concrete composite building shall be pin/rigid/semi-rigid and its rotation stiffness and moment resistance are much less than a similar RC column-to-beam connection. A semi-rigid joint is considered in this manuscript for all column-to-beam and beam-to-beam connection. The load acting on a profiled deck composite slab is typically distributed one-way in the direction of the metal deck profile. The load distribution in a RC slab depends on the direction of the main reinforcement bars. The metal deck on a profiled slab acts as a tensile reinforcement and helps to develop catenary action when the slab undergoes large deflection. A building frame overall lateral stiffness and rigidity is much high for a RC building compared to a steel-concrete composite building and thus steel building under a heavy blast acts differently with a RC building.

The computational time required for analysing the nonlinear behaviour of building frame subject to blast load or loss of critical elements is still intensive even with the use of powerful desk top computers. Kwasniewski [5] reported that the analysis of an 8-storey 3D steel building required the use of 60 processors and took 19 days to complete. Alashker et al. [6] reported that the detailed analysis of a 10-storey steel building required the use of 12 CPUs with 24 GB RAM for 2.5 days. Fu [4] also reported that the research on the behaviour of the progressive collapse of a composite building has been limited due to, (i) limited availability of analysis tools, (ii) the high cost and cumbersomeness of a full scale test, (iii) the complicated geometric models for 3D detailed numerical modelling, and (iv) the fact that a two-dimensional model does not predict the overall structural behaviour accurately and thus 3-D analysis is often needed. Many researches concentrated only on analysing small scale single storey composite building to avoid high computational cost associated with detailed geometry modelling of composite slab, joint and the complex behavioural interaction between frame components [2–3]. In addition, only limited type of moment and/or simple braced frames with or without floor slab and semi-rigid joint responses are reported in the literature. This paper attempts to fill the gap by analysing 3D building frame response under a surface blast considering the beneficial effects of floor slab and semi-rigid joints in resisting progressive collapse. A simplified composite slab model and composite joint models are adopted in this numerical investigation to reduce the computational cost. The investigation on progressive collapse of steel-concrete composite building subject to ground blast explosion was carried out using nonlinear analysis and the alternate path approach. It is recommended that nonlinear analysis should be performed for buildings subject to heavy blast loads.

2. NUMERICAL MODELLING OF STEEL-CONCRETE COMPOSITE BUILDING

A simplified composite joint and a composite slab models are adopted in the present studies to avoid detailed geometrical modelling of the structural components and to improve computational efficiency of analysing large building framework. The incorporation of semi-rigid joint model and floor slab model in 3D frame analysis tends to produce more realistic estimate of frame behaviour compared to frame model using pin or rigid joints or skeleton frame without the slabs.

2.1. BEAM AND COLUMN MODEL

Steel beams and columns are modelled using B31-two-node linear beam elements. Interaction between beam and slab is defined by tie constraint to represent the composite action between the concrete slab and steel beam. Partial composite action, i.e., slip between studs and concrete, is not considered. Partial interaction in composite beams was found to have negligible effects on the global response of 3-D frames [27]. In addition, local buckling of members is not considered, which can be avoided by using steel sections with at least Class 3 cross section [28].

2.2. COMPOSITE JOINT MODEL

A composite joint is modelled by a six degree of freedom (DOF) non-linear connector using ABAQUS [29]. The connector behaviour is represented by axial force-displacement and moment-rotation relationships. These relationships can be established using EN1993-1-8 and EN1994-1-1 component models [30, 31]. Figure 1 shows the joint components represented by a simplified joint model to be used in ABAQUS analysis. As shown in Fig. 1a, axial springs are used to represent the joint component for a slab under tension, bolt in shear, beam web in bearing and fin plate in bearing, etc. The Eurocode's component model is used to calculate the stiffness and resistance of each axial spring connector. The connectors in a joint are then assembled using two rigid bars and then analysed using the finite element analysis

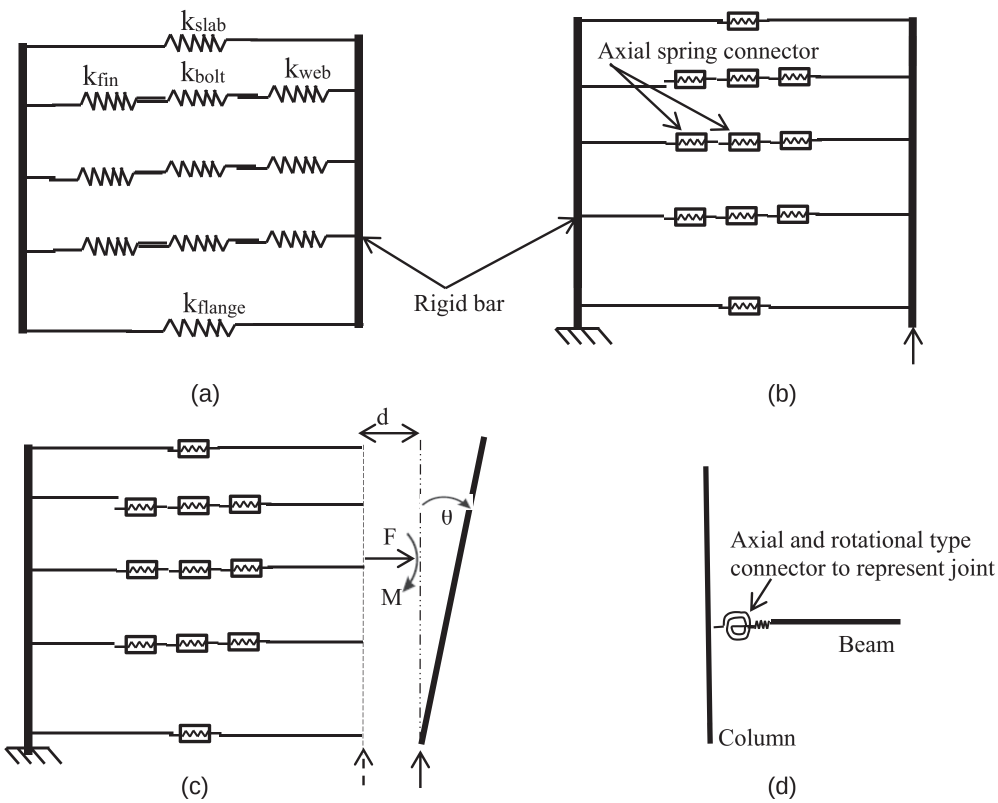

Figure 1. Model for fin-plate joint (a) Eurocode 3 component model (b) ABAQUS model (c) force-deformation relationship of joint (d) joint representation in frame analysis

software, ABAQUS, subject to axial force and moment as shown in Fig. 1c. Rigid bars represent the column and beam and each axial connector represents the joint components' axial force-displacement relation. The joint's moment-rotation (M-θ) and axial force-displacement (F-d) relationships can be calculated for frame analysis. Finally, these relations are represented by an axial and rotational connector in the analysis of the frame with semi-rigid joint, as shown in Fig. 1d. The frame analysis assumes zero joint size and neglects the effect of panel zone shear deformation in the beam to column joints [32].

The proposed composite joint model is capable of incorporating the moment-axial force coupling effect, since only the moment-rotation and axial force-displacement relationships are required to model the joints in a building frame. The design moment resistance, $M_{j,Rd}$, of a joint does not take account of any co-existing axial force in the connected member. The model should not be used if the axial force in the connected member exceeds 5% of the design plastic axial resistance of its cross section. If the axial force in the connected beam exceeds 5% of its design axial resistance, the following conservative method may be used to account approximately for the axial force and moment interaction effect on the joint:

$$\frac{N_{j,Ed}}{N_{j,Rd}} + \frac{M_{j,Ed}}{M_{j,Rd}} \leq 1 \tag{1}$$

where, $N_{j,\,Rd}$ is the axial resistance of the joint assuming no moment, and $M_{j,\,Rd}$ is the moment resistance of the joint assuming no axial force.

2.2.1. Component model of joint

EN1993-1-8 and EN1994-1 provide the guidance to calculate the steel and composite joint response analytically using the component model. Although the component model is well developed for end-plate connections, limited work is done on shear tab (fin) connections [33–37]. The moment-rotation behaviour of the fin plate connection is more complicated because the centre of compression is moving with the increase in rotation. When a fin-plate beam to column connection is subject to hogging moment, the centre of compression zone moves from the centre of the bolt group to the bottom beam flange. This means that the Eurocode's component model cannot not be applied directly to calculate the joint component's stiffness and maximum moment resistance. Therefore, a new component model for fin plate connection is proposed here as shown in Fig. 3a.

A typical four-bolt fin plate composite connection shown in Fig. 2b is used as an illustration. Figure 2a shows the force-displacement response of the axial spring. F_u is the

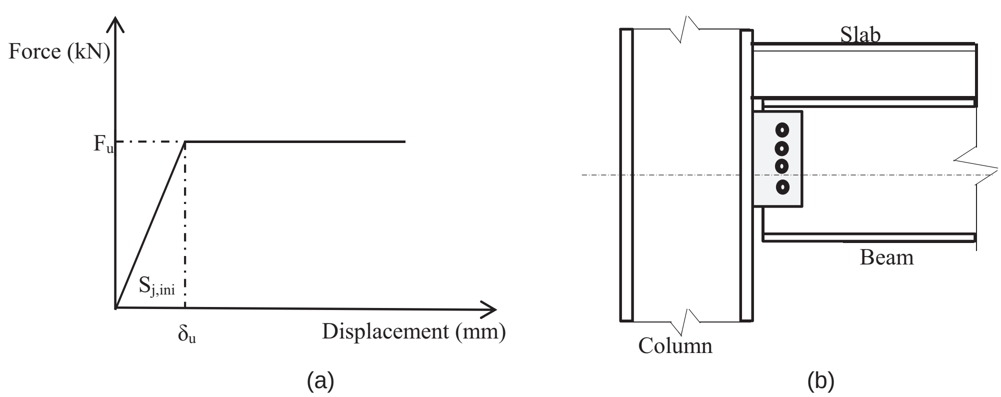

Figure 2. (a) Force-displacement of axial spring (b) typical four-bolt fin plate connection

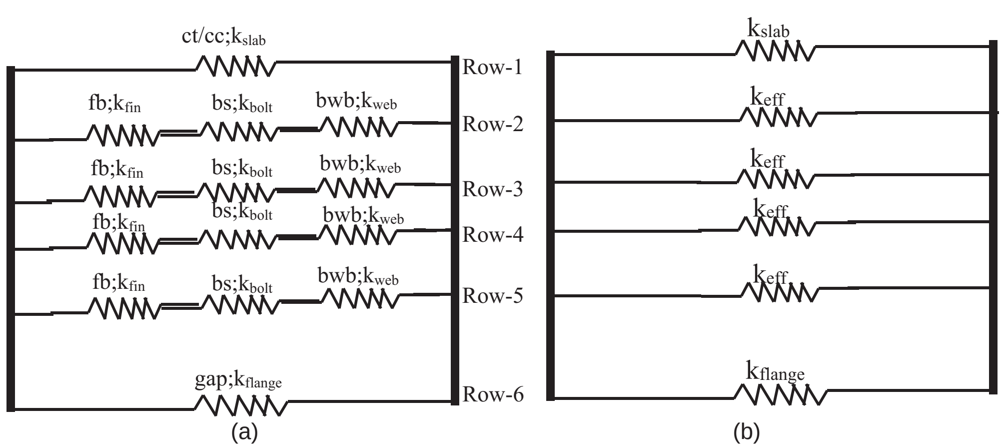

Figure 3. Component representation of composite fin plate connection

maximum force of each spring and $S_{j, ini}$ is the initial rotational stiffness. Series springs in the proposed component model are concrete in tension (ct) or concrete in compression (cc), bolt in shear (bs), fin plate in bearing (fb) and beam web in bearing (bwb). When subject to hogging moment (i.e. concrete in tension), tensile resistance of the slab reinforcement and its stiffness is in the 1st spring row, while in the case of a sagging moment (i.e. concrete in compression), concrete compressive force and its stiffness is in the 1st spring row. Row 6 spring will not be modelled for the sagging moment scenario. For the hogging moment, this spring is used to represent the gap element. k_{slab} = stiffness of slab in compression, k_{rebar} is used in case of slab in tension. k_{rebar} = sum of deck contribution and rebar contribution, k_{fin} = bearing stiffness of fin plate, k_{bolt} = shear stiffness of bolt; k_{web} = bearing stiffness of beam web, k_{flange} = represents the gap, and k_{eff} = effective stiffness of series spring of a row.

Tri-linear moment-rotation behaviour is considered for end-plate connection, as shown in Fig. 5a. Initial rotational stiffness ($S_{j, ini}$) was used as a basis to develop tri-linear moment-rotation behaviour [33]. Bi-linear moment-rotation response is derived for the fin-plate connection using the Eurocodes component model, as shown in Fig. 5b. The joint component's resistance and stiffness are firstly calculated using the component model and then the effective stiffness and effective resistance are calculated for each row. In the ABAQUS numerical model, two rigid bars (representing beam and column) are connected with axial springs (also known as connectors) as shown in Fig. 4. One rigid bar, representing the column, is fixed against displacement and rotation and the other rigid bar, representing the beam, is vertically supported and free to rotate/move at the base. The effective resistance and stiffness of the components are represented by an axial spring in a two-rigid bar model. By applying the axial fore and moment (F and M) on the rigid bar that representing the beam, the force-displacement (F–d) and moment-rotation (M–θ) relationships of a composite joint could be obtained. The rotational capacity ($\theta_{t, max}$) and spring deformation limits ($\Delta_{u, i}$) of a fin plate connection can be obtained as [2, 38]:

$$\theta_{t, max} = 0.17 - 0.00014\, d_{bg} \tag{2}$$

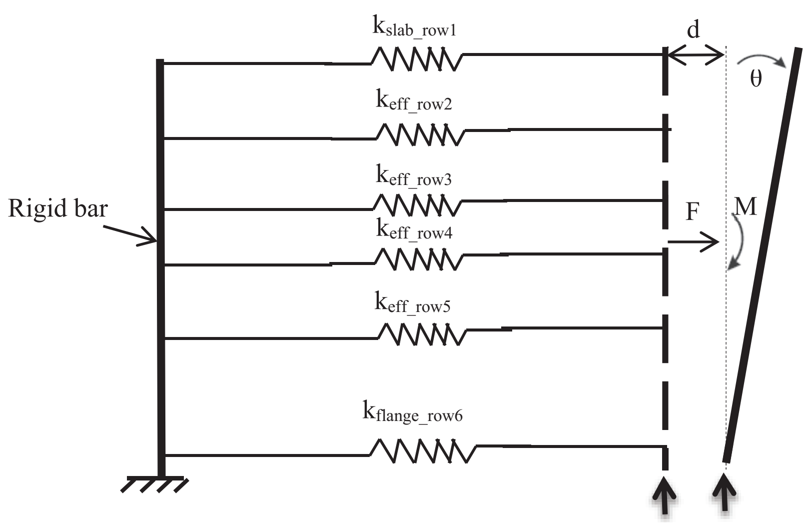

Figure 4. Spring model of fin plate connection in ABAQUS

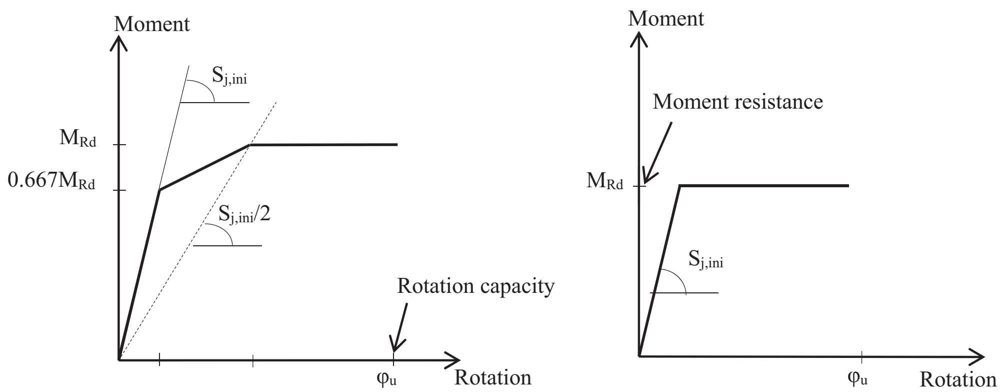

Figure 5. (a) Tri-linear moment-rotation response of end-plate connection (b) bi-linear moment-rotation response of fin-plate connection

$$\Delta_{u,\,i} = s_{max}\theta_{t,\,max} \tag{3}$$

where, d_{bg} = depth (vertical) of bolt group; s_{max} = distance from the centre of bolt group to the most distant bolt.

2.2.2. Verification study

Web-cleat connection investigated by Sadek et al. [2] is used to verify the proposed joint model. Figure 7b shows that two 6.1 m span beams were connected to a column by web-cleat connection. The web-cleat connection details are shown in Fig. 6a. The column is pushed downward under displacement control until failure of the joint. Both beam ends are assigned with pin boundary conditions. An ASTM A992 (f_y = 344.8 MPa) structural steel was used for the column and beam. The beam size was W16 × 26 and column size was W14 × 74. An ASTM A325 high strength bolt and ASTM A36 9.5 mm thick web-cleat were used for web-cleat connection. Steel beam and column material are modelled using the elastic-plastic bi-linear material model with 0.5% strain hardening with yield strength f_y = 344.8 MPa. The fracture strain of steel beam and column is taken as 0.27. The proposed joint model is adopted for column-to-beam joint. A 'slot-rotation' type connector is assigned between the

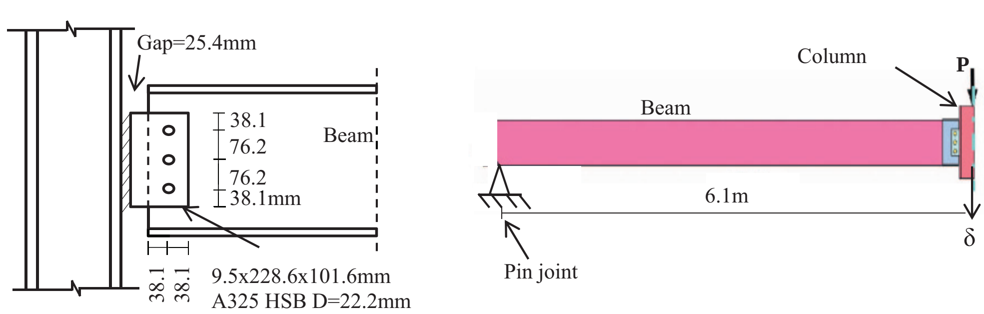

(a) (b)

Figure 6. (a) Single plate web-cleat connection (b) test half model ([2])

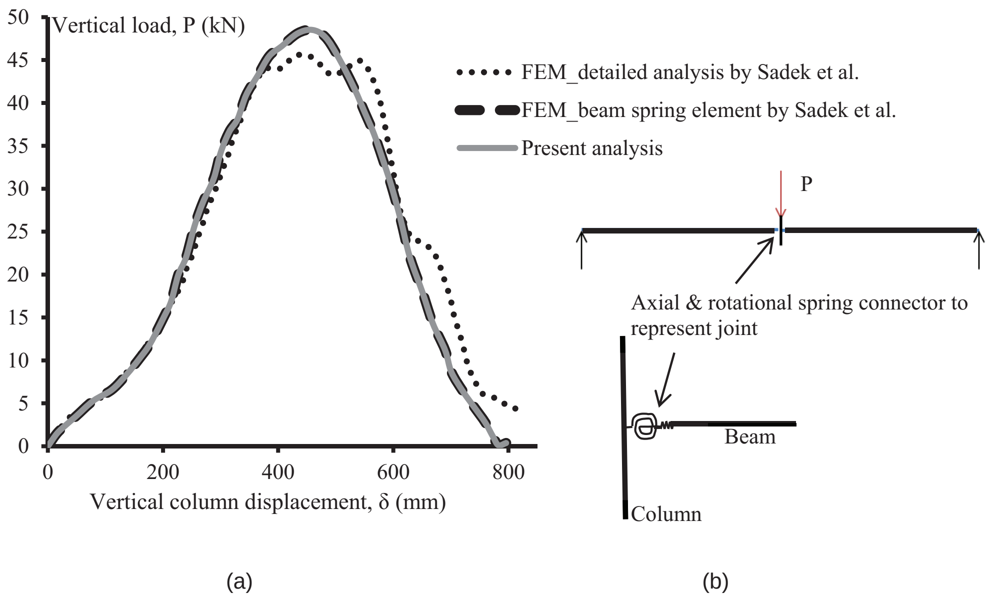

Figure 7. (a) Column vertical load-displacement (b) joint representation in FE analysis

column and beam intersection to represent the joint in ABAQUS. Joint axial force-displacement and moment-rotation relationships are assigned for the connector element based on the test data from Sarraj et al. [39]. In this verification study, a bi-linear moment-rotation relationship [(0, 0); (17.9 kNm, 0.004 rad)] is adopted and multi-linear axial force-displacement response is represented as [(0, 0); (208.3 kN, 0.2 mm); (352.9 kN, 10.6 mm); (1 kN, 45 mm)].

A nonlinear static analysis is carried out based on the proposed joint model using ABAQUS. Mesh sizes of 25, 50 and100 mm are adopted in this numerical study and the computational time is about 2-minutes. It is also found that the mesh size does not affect the web-cleat response under flexural load. Figure 7a compares the finite element analysis results from Sadek et al. [2] with the results obtained from the present analysis. The column load-displacement behaviour of the web-cleat beam-to-column test assembly is found to agree well with those obtained by Sadek et al. [2]. The proposed joint model predicts the initial stiffness, maximum resistance, failure point (displacement) and the load-displacement response of semi-rigid joints precisely. The proposed joint model avoids detailed finite element modelling of joint components and thus it reduces the computational effort. The proposed joint model is simpler as compared to the finite element modelling of joints proposed by Sadek et al. [2] and it is accurate enough in predicting the joint response with less computational effort.

2.3. COMPOSITE SLAB MODEL

A simplified composite slab model is proposed to avoid complicated geometry modelling of the profile composite slab and to reduce the computational time required for analysing the 3–D large scale framework. The profile metal deck is represented by rebars in a longitudinal direction based on equivalent area of the respective web and flange plates of the metal deck, at which rebar is assigned at the centre of each metal deck strips. Profile concrete is converted into an equivalent uniform concrete section and it is modelled using a four-node homogeneous shell element with reduced integration (S4R). Rebar is defined using rebar definition through the ABAQUS library. The proposed simplified composite slab model is shown in Fig. 8. The profile concrete in the composite slab as shown in Fig. 8a is converted into an equivalent concrete slab with uniform thickness, D_S–$D_P/2$, as shown in Fig. 8b. Metal deck strip areas A_1, A_2 and A_3 are calculated by multiplying the deck thickness by its strip length. The rebar area becomes, $a_1 = A_1$, $a_2 = A_2$ and $a_3 = A_3$. The composite slab will be converted into an equivalent uniform reinforced concrete section using the proposed simplified slab model and thus the equivalent concrete section could be modelled using a shell element, and rebar could be represented by the rebar option in ABAQUS. The membrane force is not affected since the area of metal deck and concrete are the same.

A slab model with an equivalent second moment area is compared against the proposed slab model, which is based on an equivalent area of steel and concrete. It is observed that the effect on global response of frame (e.g. deflection) is not significant since the slab is compositely modelled with a steel beam. The composite beam stiffness is not significantly affected by the small changes in depth of the concrete and the exact position of rebar. Alashker et al. [3] reported that increasing the slab reinforcement did not change the frame load-displacement behaviour significantly. The simplified slab model is proposed based on assumptions that (i) perfect bond between the concrete and metal deck and the slip between concrete slab and metal deck will not significantly affect the global response of the frame [27], (ii) stiffness of the metal deck in the orthogonal direction is negligible and can be ignored, (iii) inelastic behaviour of each composite slab components (concrete, metal deck and rebar) can be defined by their respective material stress-strain relationships and the small error, due to the change of depth of bottom deck area A_3, is negligible. This model is different from that used by Alashker et al. [6], who assumed that the rebar area = 50% of metal deck area and that the rebar area was defined at the centreline of the slab, and (iv) embossment on the metal decking is not taken into consideration in calculating the area and second moment of area of deck.

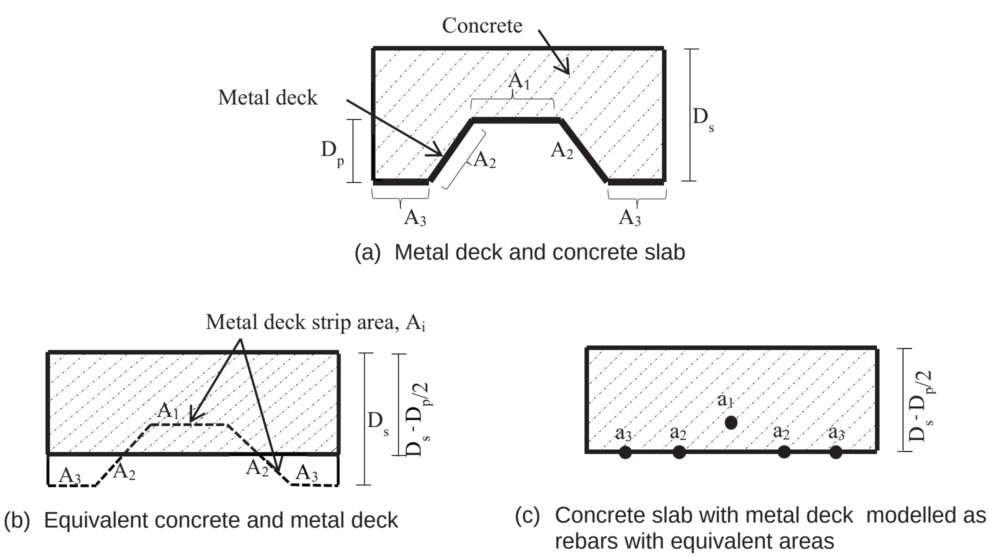

(a) Metal deck and concrete slab

(b) Equivalent concrete and metal deck

(c) Concrete slab with metal deck modelled as rebars with equivalent areas

Figure 8. Proposed simplified composite slab model

2.3.1. Verification study I: Composite slab under bending

A composite slab tested by Easterling and Abdullah [40] is referred to study the composite slab response under flexural load. Schematic test setup is shown in Fig. 9. Properties of concrete and steel sheeting are summarised in Tables 1 and 2. Test and FEM results from Easterling and Abdullah [40] are compared with the results obtained from the proposed simplified slab model as shown in Fig. 10. ABAQUS explicit dynamic analysis is used to predict the composite slab response.

Concrete material is modelled using the concrete damage plasticity model in ABAQUS with the concrete tensile strength of 10% of compressive strength. Compressive strength of concrete is indicated in Table 1. Mesh size of 10 mm is adopted. Load is slowly applied by means of the smooth amplitude function to ensure a quasi-static loading (2-seconds, 5-seconds and 20-seconds are used). Computational time for 5-seconds simulation time is about 2.5 hours and the computational time for 20-seconds simulation time is about 2 days for the mesh size of 10 mm.

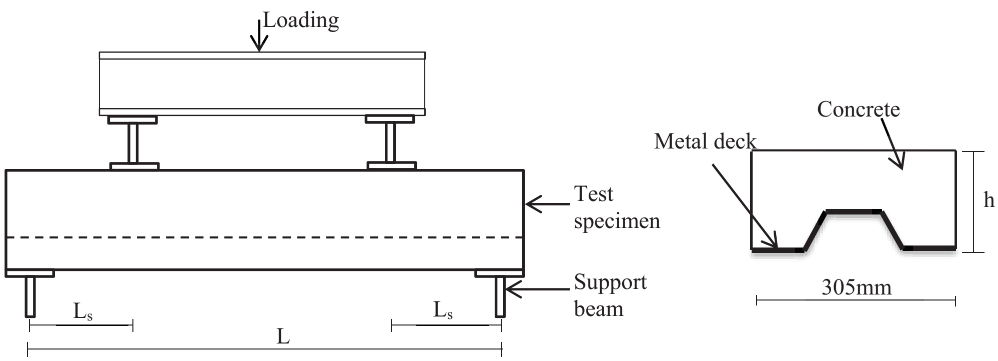

Figure 9. Bending test specimen ((40))

Table 1. Test specimens and parameters ((40))

Specimen	Deck depth (mm)	Deck thick (mm)	f_y (MPa) Yield stress	f_u (MPa) Ult. stress	Specimen length, L (mm)	Shear span, L_s (mm)	Concrete thickness, h (mm)	Conc. comp strength f'_c (MPa)
5	76	1.5	350	410	1220	410	190	35

Table 2. (a) Steel properties (b) concrete properties ((40))

(a)

Steel properties	**Values**
Density	7800 kg/m^3
Elastic modulus (flanges)	203.4 GPa
Yield stress (flanges)	345 MPa
Elastic modulus (web)	101.7 GPa
Yield stress (web)	173 MPa

(b)

Concrete properties	**Values**
Density	2400 kg/m^3
Elastic modulus	24.8 GPa
Poisson ratio	0.2
Cracking failure stress	2.07 MPa

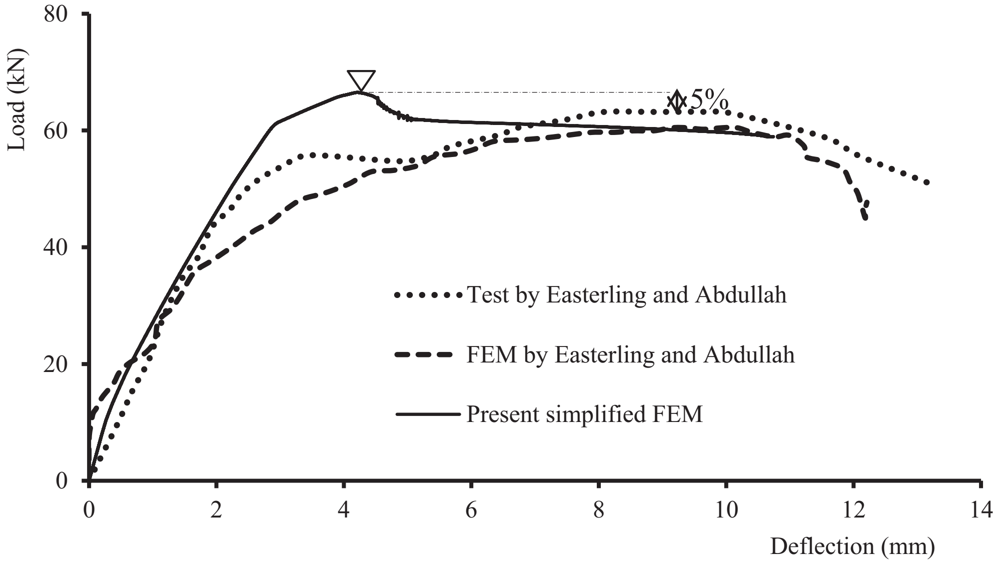

Figure 10. Load-mid span deflection for specimen S5

The discrepancies between the test result and the predicted numerical results are mainly due to the assumption of perfect bonds between the concrete and the metal deck, which results in over-prediction of the initial stiffness and strength of the specimen. Insufficient details of the materials are reported in Easterling and Abdullah [40] and thus the Eurocode-2 concrete material model ([41], [42]) is adopted in this verification study. Concrete damage plasticity model, using Eurocode-2 is adopted here to define both the compression and tensile behaviour of concrete in ABAQUS. The Eurocode-2 concrete material model overestimates the strength of the test specimen. Both the above mentioned combined effects (of using the perfect bond and the Eurocode-2 material model) affect the accuracy of results by 5% compared to the test result. The numerical models are sufficiently refined and they are not the reason for the discrepancies between test and numerical analysis.

FEM analysis by Easterling and Abdullah [40, 43] predicts the maximum resistance of the composite slab specimen reasonably well, but it does not capture the initial stiffness of the composite slab compared to the test result. However, the proposed simplified composite slab model captures both the initial stiffness and the maximum resistance of the composite slab reasonably well. The predicted maximum resistance of composite slab is within 95% accuracy compared to the test result, which is acceptable in this investigation due to the complicated geometry and complex interaction response of composite slab. Detailed modelling of the non-linear interactive behaviour between steel deck, rebar and concrete slab of a composite slab requires much computational time and effort to capture the interaction between the concrete slab and the steel components. The proposed slab model avoids detailed geometric modelling of metal deck profile and requires less computational time for analysing a large building frame.

2.3.2. Verification Study II: Composite beam under flexural load

Composite beam specimen CB2 tested by Ranzi et al. [44] is used as reference to validate the FE model of composite beam under flexural load. A 130 mm thick, 2000 mm wide composite slab was connected to an Australian standard beam 410UB54 with length = 8.050 m. Two shear studs per through were welded on the beam. The shear studs are 19 mm diameter and, after welding, have a height of 115 mm above the steel deck. The test set-up is shown in Fig. 11a. The beam was tested by applying loads at 16 points along the beam length to simulate uniform load. Mesh size of 50 mm is adopted for the simplified FEM. Load is applied slowly by means of the smooth amplitude function to ensure a quasi-static loading. Computational time for simplified FE analysis is about 1-hour for preliminary analysis and the simplified FE analysis consumes about 12-hours for 10-seconds loading time. Simplified numerical model in ABAQUS is shown in Fig. 11b. The test result from Ranzi et al. [44] is compared with the result obtained from the simplified finite element model as shown in Fig. 12.

The proposed simplified finite element model captures initial stiffness and maximum resistance of the composite slab reasonably well compared to the test result. The simplified

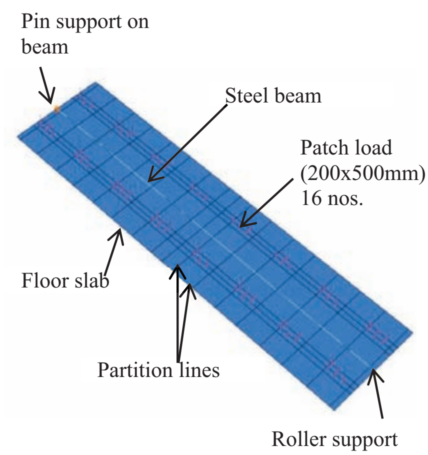

(a) (b)

Figure 11. (a) Test setup ([44]) (b) simplified FE model in ABAQUS

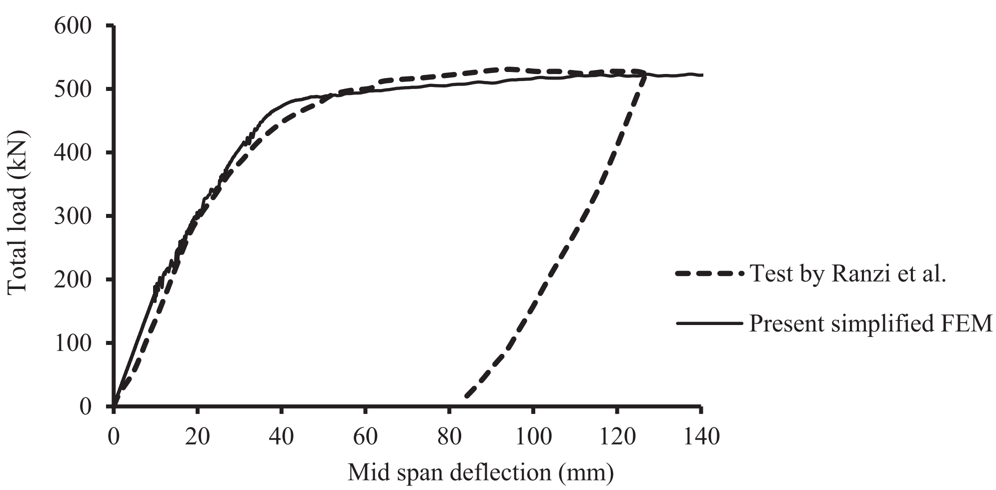

Figure 12. Total applied load – mid span deflection of beam CB2

finite element model (FEM) avoids detailed geometry modelling of the composite beam and reduces the computational time. On the other hand, 3D finite element modelling of the composite beam is rather tedious and has involved other structural components including interaction between steel deck, rebar, beam and concrete slab. The proposed slab model is accurate enough in predicting the composite slab behaviour with less computational effort. Similar validation studies have been carried out on other test specimens and the results are not shown herein.

3. ROBUSTNESS ANALYSIS OF 3-D COMPOSITE FRAME SUBJECT TO BLAST LOAD

3.1. ALTERNATE PATH APPROACH

The Alternate Path (AP) approach, which is a threat independent methodology, is commonly used as a design guide for minimising the potential for progressive collapse [7, 45]. This approach would generally require the removal of single member (column or beam) regardless of threat type, although the method does not exclude the possibility of removing more than one member. The Alternate Path approach is performed to ensure the bridging capability of structure over a missing structural element under localised damage. Non-linear dynamic (ND) analysis may be required to predict accurately the response of building structures subjected to extreme load since large deflection beyond the elastic limit is expected and sudden column loss will often induce dynamic load [7].

3.2. NONLINEAR DYNAMIC ANALYSIS

An integrated nonlinear dynamic analysis involving blast analysis and fibre-element modelling of structural members including member initial imperfections would involve huge computational resources and may not be practical for the analysis of large scale multi-storey composite building frames. In the proposed two-step process, a nonlinear dynamic analysis is firstly carried out on 3D composite framework subject to blast load based on the proposed simplified joint and composite slab models, if applicable. Damaged members are then identified by checking the member forces against their maximum resistance. The damaged members are then removed for subsequent collapse analysis. The proposed two-step process is proposed for practical implementation as it involves less computational time and less effort in modelling.

Nonlinear dynamic analysis may be carried out by considering the blast to occur at any floor level within a building or at a standoff distance from the building. Critical structural elements in the building may be identified by considering the various blast scenarios. Blast pressure-time history due to an explosion may be obtained from TM-5-1300 guideline and the dynamic loads are applied for blast analysis of a building. The nonlinear analysis is performed to identify the damaged/incapable elements/members in the building frame. The structural element is considered as damaged/incapable, if the demand on a structural element exceeds its resistance or the prescribed limits such as rotation capacity or ductility limit [7]. The structural element damage criteria may be governed by the respective resistance to axial force, bending moment, shear force, or a combination of these, or may be due to limit of deflection or rotation at accident limit states.

After the removal of the damaged members, subsequent non-linear dynamic analysis is performed on the damaged building frame. The residual resistance of the removed member is ignored and it will generally lead to conservative estimate of the progressive collapse resistance of the structure. The collapse analyses are performed here using ABAQUS explicit solver with a desktop computer of one CPU (6-processors) and 12GB RAM. Computational time for typical ten-storey steel-concrete composite building frame, which has five bays in each direction, is around one to two days depending on finite element mesh size, material model, size of time increments, etc.

4. CASE STUDY: TEN-STOREY COMPOSITE BUILDING SUBJECT TO A SURFACE BLAST

4.1. ALTERNATE PATH APPROACH

A ten-storey special moment frame (SMF) with reduced beam section (RBS) previously studied by Alashker et al. [6] is modified herein for robustness analysis, as shown in Fig. 13a. The same ten-storey steel building with (i) diagonal braces at corners (ii) centre core wall (iii) rigid moment joints were investigated using alternate path approach (AP) for corner column (CC), perimeter column (PC) and internal column (MC) loss. Non-linear dynamic (ND) analyses were performed according to the General Service Administration guideline [7]. The ten-storey building foot print dimension is 30.5 m × 45.7 m. The column spacings in the longitudinal and transverse directions are 9.14 m and 6.1 m, respectively. Beam and column sizes are shown in Fig. 13a. A secondary beam, W14 × 22, is not shown in Fig. 13a for clarity. The composite floor slab consists of a 82.5 mm thick lightweight concrete topping (concrete density = 17.3 kN/m^3) on a 76.2 mm deep metal deck. Metal deck thickness is 0.9 mm and nominal concrete strength is 20.7 N/mm^2. The slab is lightly reinforced with wire mesh (1.4 mm diameter and 152 mm spacing in both directions). Self-weight of floor is 2.2 kN/m^2. Super-imposed dead load of the typical floor is 1.44 kN/m^2 and the roof is 0.48 kN/m^2. Live loads of the typical floor and the roof are 4.79 kN/m^2 and 0.96 kN/m^2 respectively. All the beam and column sections have the same steel grade with yield strength, tensile strength and modulus of elasticity equal to f_y = 345 MPa, f_u = 448.2 MPa, and E = 200 kN/mm^2. For the simple braced frames, the beam-to-column connections are fin-plate types made by welding a 9.5 mm thick single shear plate of A36 steel to the column and bolted to the beam web using 3 numbers 22 mm diameter A325 high strength bolts, as shown in Fig. 14a. Yield strength and tensile strength of these bolts are 634 MPa and 827 MPa respectively. The shear plate yield strength and tensile strengths are equal to f_y = 248 MPa and f_u = 421 MPa. Numerical modelling of composite joint and slab in a frame are reported in Section 2.

For the core braced simple frame, 300 mm thick concrete walls are used to form the central core (between grids C–D and 3–4) to provide lateral load resistance to the simple frame surrounding the central core, as shown in Fig. 13b. The core wall is reinforced by two layers of T16-300 steel bars arranging in both way with concrete cover of 30 mm. Shell elements (S4R) are used to model the core wall.

Concrete material is modelled using the concrete damage plasticity model in ABAQUS and tensile strength of concrete is neglected. Steel material is modelled using the elastic-plastic bi-linear material model with 0.5% strain hardening. The fracture strain is taken at 0.27 plastic strain as in Alashker et al. [6]. The material model for metal deck and rebar is assumed to be elastic-perfectly plastic with f_y = 248 MPa and fracture strain 0.25. Structural damping of 5% is assumed.

As reported, shell elements (S4R) used for slab, and beam elements (B31) used for columns and beams in the numerical modelling using ABAQUS. Full composite action is defined between slab and beam using tie constraints. Finite element mesh size of 500 mm is adopted in this comparison study. The simple connections are assumed to be fin-plate bolted connections, as shown in Figure 14a. Figure 14b and 14c show the fin-plate connection axial force-displacement and moment-rotation relationships used for the simple connections in this analysis (for the case of a metal deck parallel to the beam).

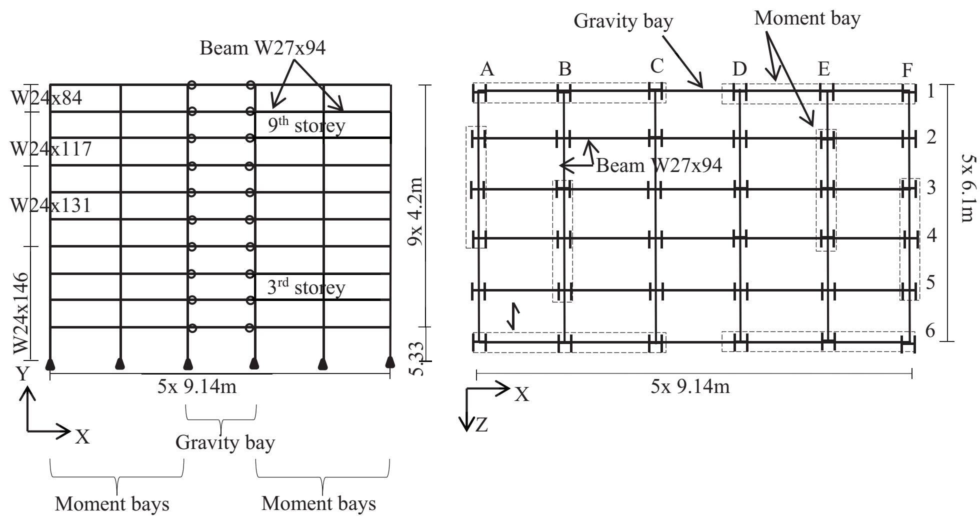

(a) Elevation and plan view of special moment frame ([6])

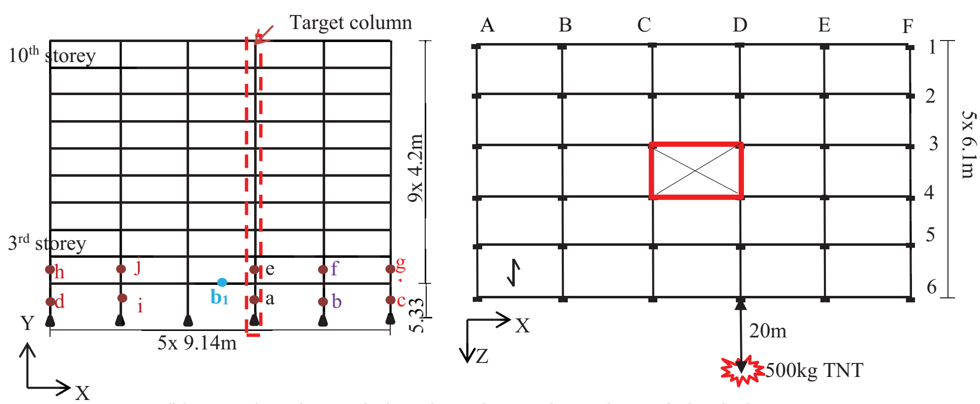

(b) Elevation and plan view of central core braced simple frame

Figure 13. Elevation and plan view of ten-storey building (secondary beams are not shown)

4.2. NONLINEAR DYNAMIC ANALYSIS

The ten-storey centred core building frame, which is reported in Section 4.1 and Fig. 13b is investigated for a surface bomb blast of 500 kg TNT, which is detonated at 20 m away from the building front column D6 (along the grid D). The US guideline TM-5-1300:1990 ([8]) is used to predict the blast pressure-time history for the numerical analysis. A nonlinear dynamic analysis is firstly performed to identify the possible damaged elements in the building frame for the collapse analysis. Since the explosion occurred at 20 m away from the structure, the blast load acting on the top and bottom surface of the beam and slab are almost the same and thus uplift force is neglected. However, in the case of nearby explosion, the uplifting loads on the beams and slabs must be considered as they can generate an uplifting initial velocity and displacement [10]. In the present study, the blast loads are applied on the front face of the ten-storey building front columns as uniform distributed load, based on the

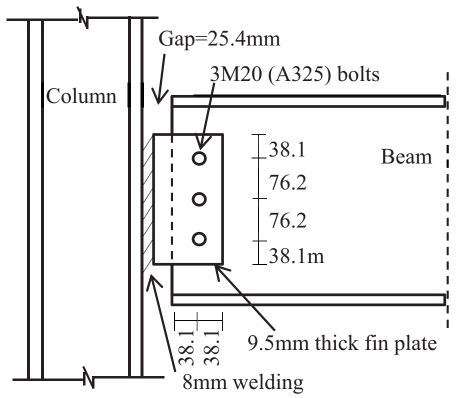

(a) Fin plate connection

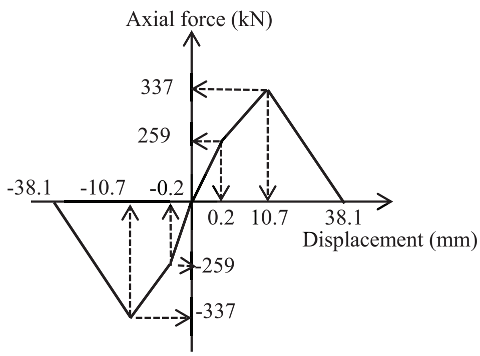

(b) Axial force-displacement of fin-plate connection

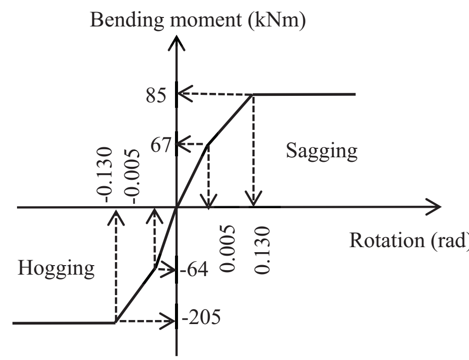

(c) Moment-rotation of fin-plate connection

Figure 14. Fin-plate connection, axial force-displacement and moment-rotation relationship of fin-plate connections

assumption that the external claddings are fragile and only the width of column width + 200 mm is effective in attracting blast pressure [46]. Similar approach was used by Shi et al. [10] in their numerical analyses. The building frame is subjected to a gravity load combination: 1.0 × dead load + 0.25 × live load in load step 1. A 500 kg TNT is detonated at a distance of 20 m away from the target column D6 at 1.5 seconds from the initial time, which is represented in load step 2. Blast pressure-time history for each storey column is calculated using TM-5-1300 and it is applied as uniform distributed load appropriately at load step 2. Applied load-time relationship is shown in Fig. 15. The frame response is monitored for three seconds. Few critical locations on column and beams are monitored. Among them, monitoring points ‘a’ to ‘j’ are at mid-height of the 1st and 2nd storey columns and the monitoring point ‘b_1’ is at mid-point of the 1st storey beam. Building frame schematic views and monitoring points are shown in Fig. 13b (secondary beams are not shown for clarity).

Mechanical properties of the steel and concrete materials are affected due to the dynamic blast load ([8, 11, 47]). TM-5-1300 (1990) states that a structural element subjected to a blast loading exhibits a higher strength than a similar element subject to a static loading. This increase in strength, for both the concrete and steel, is attributed to the rapid strain rates that occur in dynamically loaded members. These increased stresses or dynamic strengths are

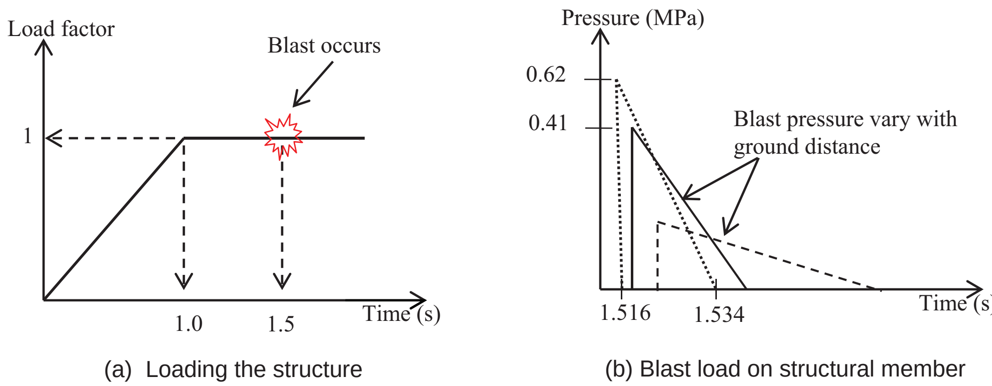

Figure 15. (a) Gravity load application on frame (b) blast loading-time relation

used to calculate the elements of dynamic resistance to the applied blast load. Thus, the dynamic ultimate resistance of an element subjected to a blast load is greater than its static ultimate resistance. Both the concrete and steel exhibit greater strength under rapid strain rates. The higher the strain rate, the higher the compressive strength of concrete and the higher the yield and ultimate strength of the steel. Therefore, strain rate effect due to blast is considered in the numerical analysis. The dynamic design yield stress of steel ($f_{y,\,dynamic}$) is given by:

$$f_{y,\,dynamic} = a\left(DIF\right) f_{y,\,static} \tag{4}$$

where, DIF = dynamic amplification factor; $f_{y,\,static}$ = static yield stress of steel. 'a' is a modification factor that takes into account the fact that the yield stress of a structural component is generally higher than the minimum specified value given in the code. The value of a = 1.1 is recommended. The DIF value for concrete is taken as 1.25 for bending. For steel, the DIF is taken as 1.10 for yield strength and 1.05 for ultimate tensile strength. Similar approach was used by Fu [47] to account for the mechanical properties of material under dynamic loading. Concrete material is modelled using the concrete damage plasticity model in ABAQUS and tensile strength of concrete is neglected. Steel material is modelled using the elastic-plastic bi-linear material model with 0.5% strain hardening. The mechanical properties of the steel and concrete materials are affected due to the dynamic blast load and thus dynamic design stress of steel and concrete are defined by stress-strain relationships for each elements (concrete, steel, metal deck, rebar) instead of defining their static stress-strain relationship.

4.2.1. Effect of standoff distance

The front columns of the building facing the blast are arranged in such a way that they bend about their minor axis when subject to blast pressure. Figure 16 shows the graphical views of a 3D deformed building frame under the AP approach (single column loss) and nonlinear dynamic analysis (five column damage and loss). With reference to the monitoring points depicted in Fig. 13b, the effect of standoff distance on nonlinear dynamic analysis is summarised in Figs. 17 to 20 and Tables 3 and 4. The axial force, bending moment, shear force and deflection responses of the 1st storey perimeter columns D6, E6 and F6 are

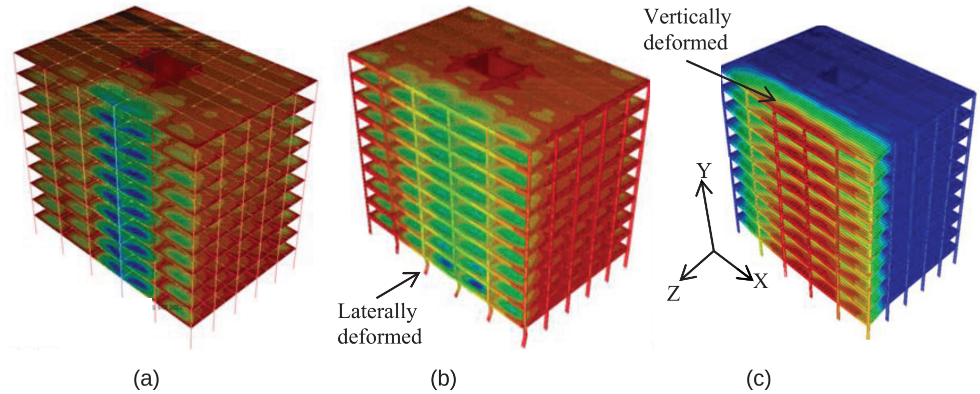

Figure 16. Deformed frame view for (a) one-column loss AP analysis (b) nonlinear dynamic analysis (c) five-column loss collapse analysis

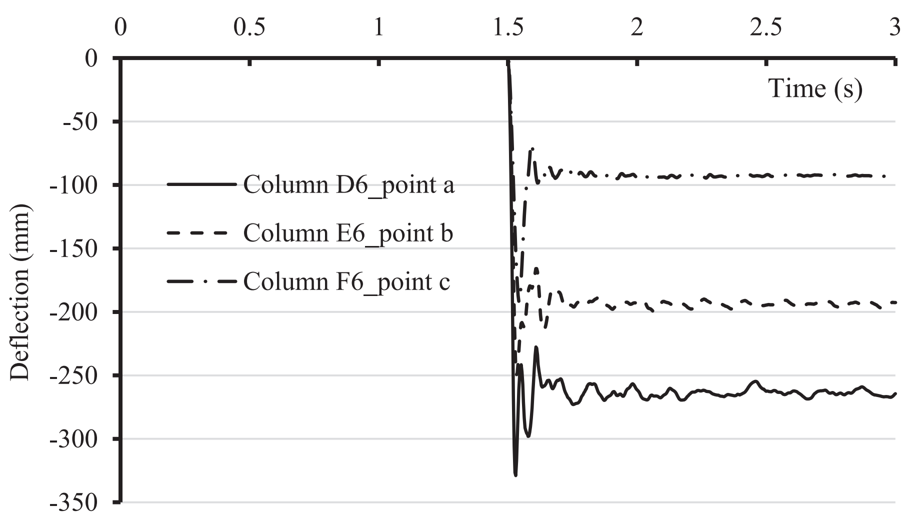

Figure 17. Column lateral deflection (dir-Z) in nonlinear dynamic analysis for 5% damping

summarised in Figs. 17 to 20. The numerical results clearly show that blast effect on adjacent structural member is severe compared to a structural member that is further away from the blast location. Significant axial force (AF) variation in a column is observed due to the high lateral blast pressure. Shear force induced by the direct blast is within the column shear resistance. The maximum axial force, bending moment and shear force on 1st storey columns due to blast can be three times higher than the force before the blast. Nonlinear dynamic analysis results show that many 1st storey perimeter columns reached the plastic moment resistance. Analysis results show that lateral deflection of 1st storey columns due to blast is not negligible. Large deflection may damage the column with regard to support rotation, member ductility, second order effect etc.

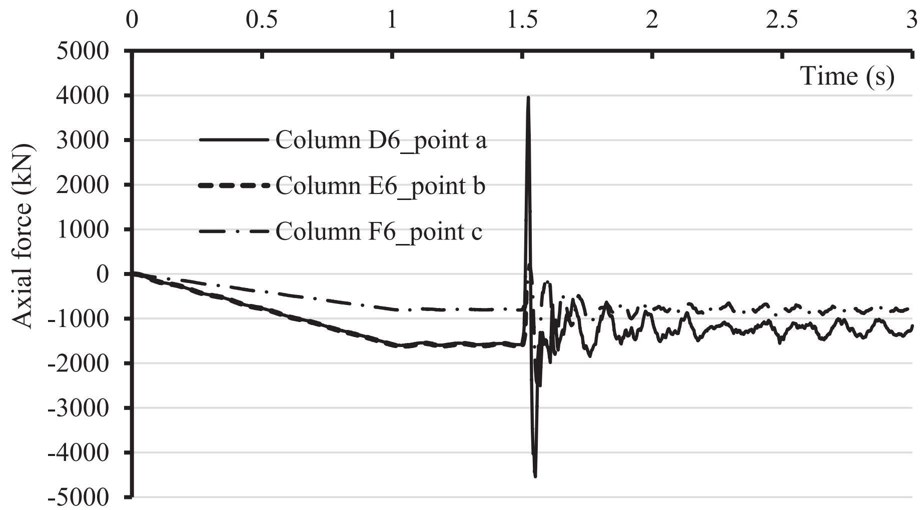

Figure 18. Column axial force in nonlinear dynamic analysis for 5% damping

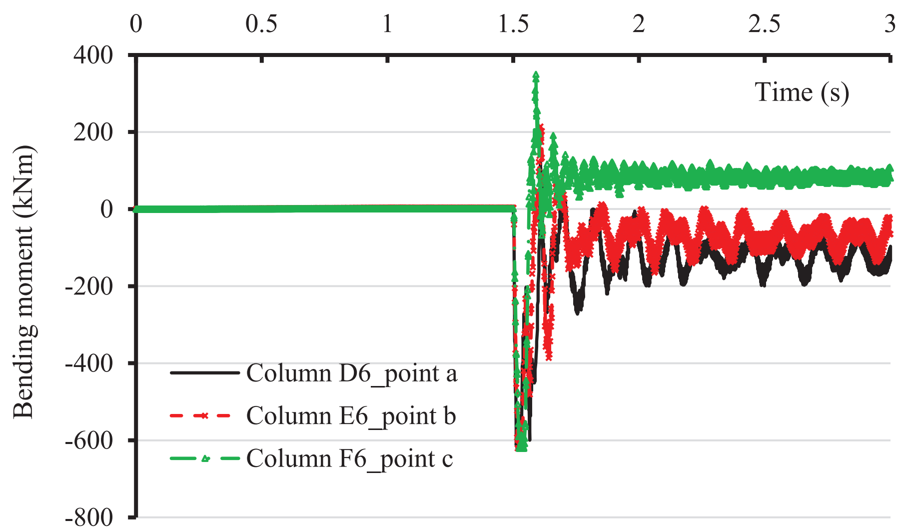

Figure 19. Column bending moment in nonlinear dynamic analysis for 5% damping

Beam/column rotation contour (UR1) due to the blast at end of the nonlinear dynamic analysis (t = 3sec) is shown in Fig. 21a (floor slab is not shown). UR1 means rotation about axis-1(U_1 means deflection in axis direction-1). Analysis results show that the moments and axial force acting on the five front perimeter columns (B6, C6, D6, E6 and F6) at the first storey due to blast load reach the member buckling resistance as shown in Table 3 and they are treated as damaged and removed in the subsequent collapse analysis. The residual resistance of the damaged member is ignored and this will generally lead to conservative estimate of the progressive collapse resistance of the structure. The plastic strain of these five

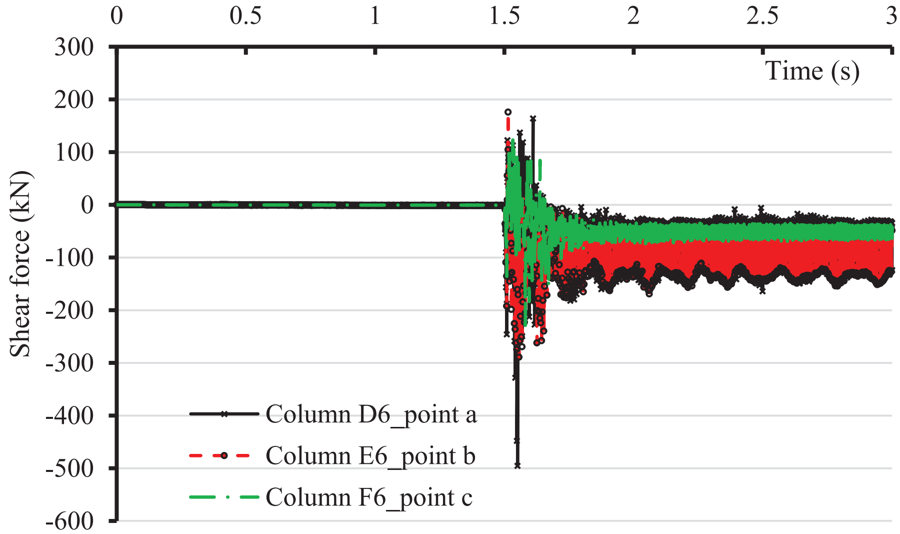

Figure 20. Column shear force in nonlinear dynamic analysis for 5% damping

Table 3. Lateral deflection and force demand of building frame for 5% damping with strain rate effect

Point	Max. lateral deflection (mm) (Z-direction)	Max. minor axis bending moment (kNm)	Max. axial force (kN)	Max. shear force (kN)	Max. plastic strain
a	−329	621*	4542	496	0.031
b	−250	621*	3799	289	0.031
c	−192	621*	2448	229	0.018
d	−86.8	537	1323	143	0.001
e	−93.5	477	4029	313	0.001
f	−61.4	420	3502	260	0
g	−69.7	304	2279	233	0
h	−52.6	252	1180	229	0
i	−144	621*	2698	296	0.014
j	−43.0	386	2467	252	0
b_1	−6.49	65.4	849	150	0

* Plastic moment resistance is reached

columns are varies within the 0.014 to 0.031, as summarised in Table 3, and they less than the defined fracture limit of 0.27. Figures 22 and 23a show the deflection history at column D6 (point-a). Figure 22 shows that the vertical deflection predicted by the AP approach (due to perimeter column D6 loss) is higher than from the nonlinear dynamic analysis. Subsequently, collapse analysis is required to be executed with the absence of the damaged element to complete the progressive collapse analysis. Nonlinear dynamic analysis results are summarised in Tables 3 and 4 for frame with strain rate effect. Figure 23b shows the axial force (AF) and shear force (SF) demand at monitoring column D6 (point a) in the nonlinear

Table 4. Maximum deflection and forces for building frame for 5% damping with strain rate effect

Point	Max. lateral deflection (mm) (X-direction)	Max. vertical deflection (mm) (Y-direction)	Max. major axis bending moment (kNm)	Max. torsional moment (kNm)	Max. major axis shear force (kN)
a	92.6	–23.1	163	35.4	88.9
b	40.8	–13.8	197	20.9	78.7
c	19.1	–8.38	276	13.2	93.8
d	6.89	–2.01	245	22.7	74.9
e	11.4	–38.0	180	27.6	152
f	8.61	–21.7	225	15.5	102
g	9.27	–11.8	155	12.4	152
h	6.29	–3.55	203	16.7	98.4
i	9.15	–5.23	173	14.5	46.7
j	3.75	–8.29	147	11.9	57.7
b_1	4.83	–50.1	861	1.57	124

dynamic analysis. High demand of force occurred, especially, axial force at the instance of blast pressure hitting the building, which can only be obtained by the nonlinear dynamic analysis.

4.2.2. Effect of strain rate

Building frames with 5% damping and without strain rate effect analysis results are summarised in Table 5. Analysis results show that the beneficial effect of strain rate considerably affects the analysis result (e.g. deflection, forces, capacity and plastic strain) and the results are summarised in Tables 3, 4 and 5. The deflection (vertical and lateral) of frame with strain rate effect is less than the deflection of frame without strain rate effect and also, the force demand of frame with strain rate effect is higher than the force demand of frame without strain rate effect. This is because the dynamic properties of materials are higher than the static properties of materials (TM-5-1300) (e.g. Young modulus, yield stress, ultimate stress, and concrete compressive strength). It means dynamic strength and stiffness increase due to strain rate effect and causes more force and less deformation compared to static response. It is also observed that there is no significant effect in blast analysis result by damping.

4.3. COLLAPSE ANALYSIS

In the second stage of the two-step analysis, the identified damaged perimeter columns (B6, C6, D6, E6, and F6) are suddenly removed at 1.5 seconds from the building frame in subsequent collapse analysis. The five 1st storey columns' supports are suddenly removed to simulate the five column loss due to the blast. An alternate path approach is performed with the removal of a single column (D6). For the parametric study, a three-column loss scenario (C6, D6, and E6) is investigated. Analysis results for single column loss (AP), three column loss (for parametric study) and five column loss (according to the nonlinear dynamic analysis) are compared. Lateral deflection for a three column loss collapse analysis is shown in Fig. 21b. Lateral deflection due to a three column removal is less than the lateral deflection

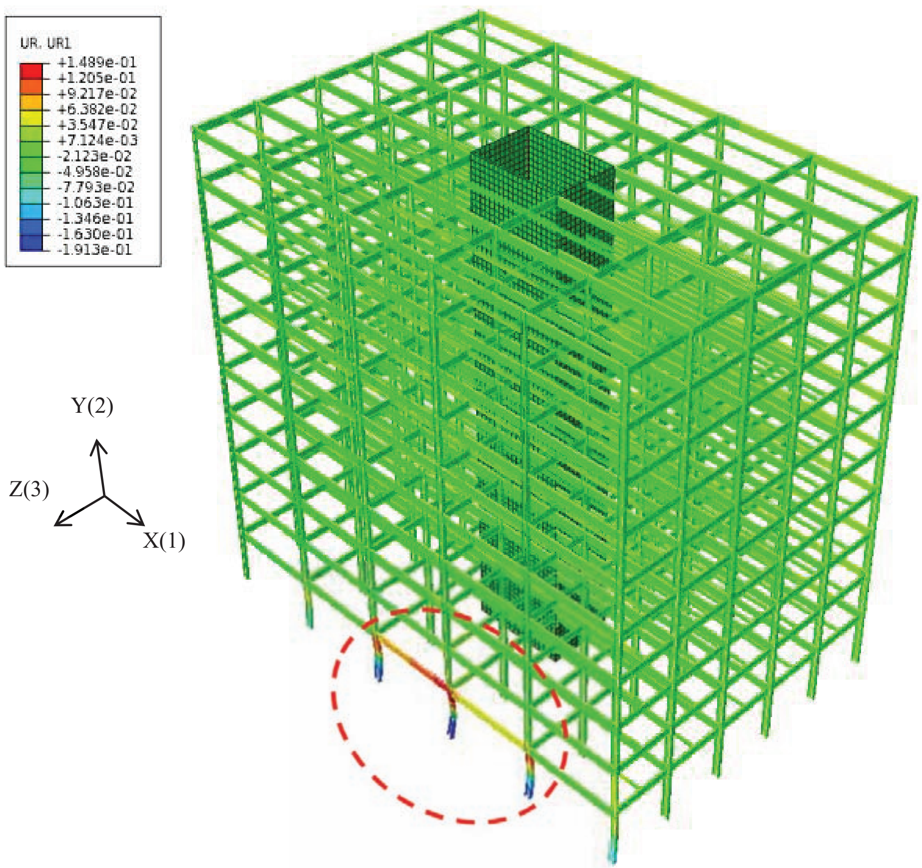

(a)

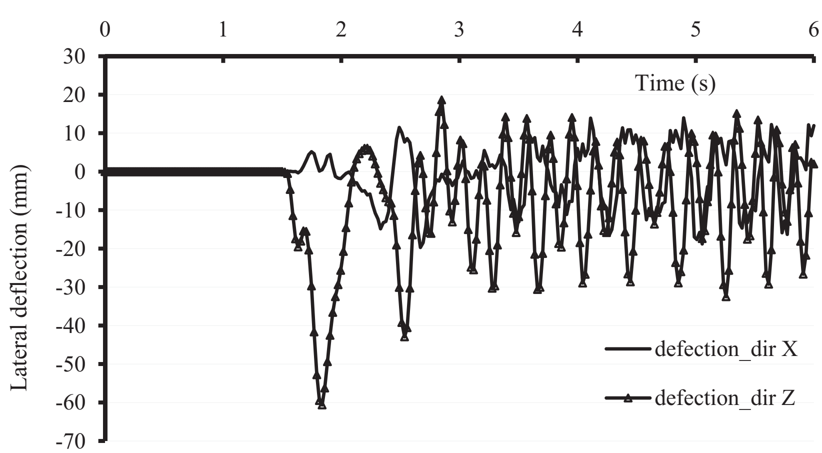

(b)

Figure 21. (a) Rotation contour UR1 (b) lateral deflection at column D6 for 3-column loss collapse analysis

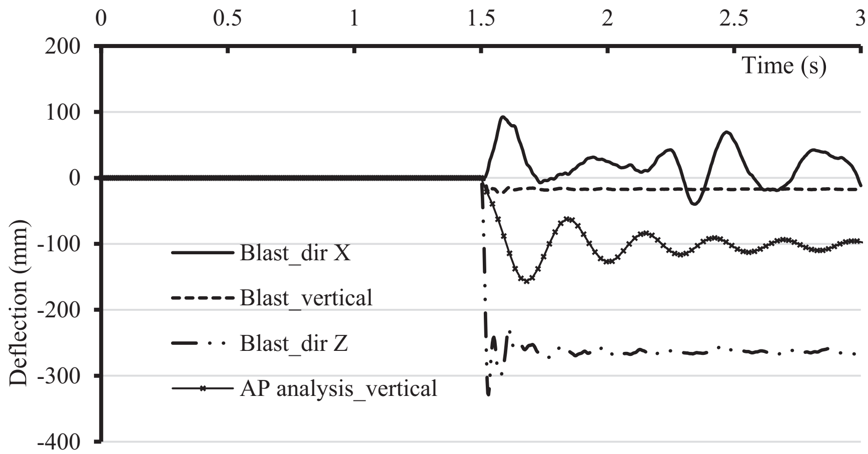

Figure 22. Deflection at mid height of the column D (point-a) with time

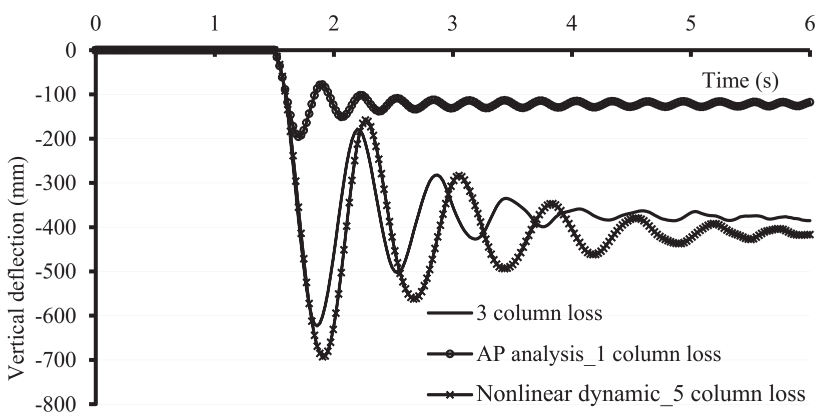

(a)

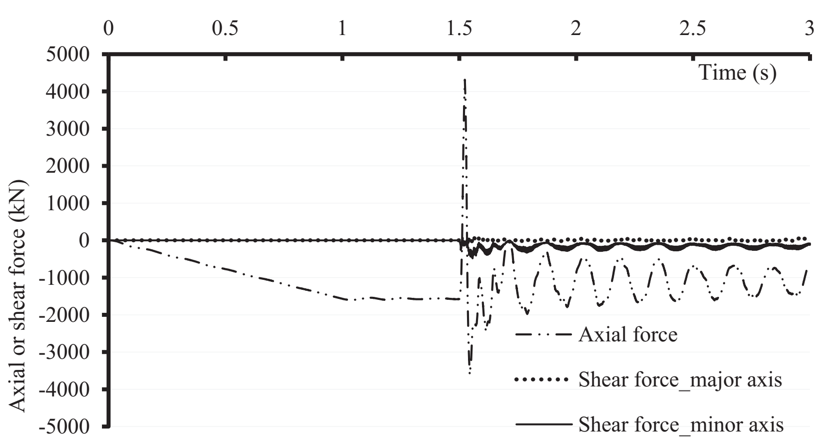

(b)

Figure 23. (a) Deflection of frame (b) column D6 (point a) force variation with time due to blast for 5% damping

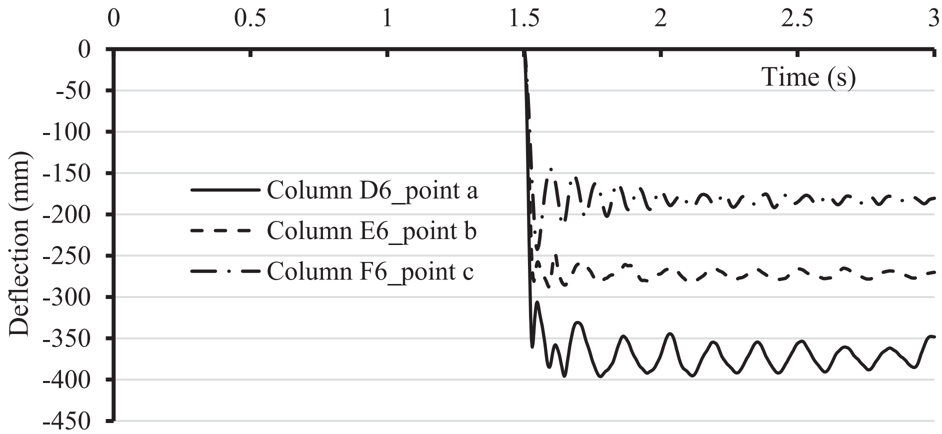

Figure 24. Column D6 lateral deflection (dir-Z) in nonlinear dynamic analysis for no-damping and without strain hardening effect

in a nonlinear dynamic analysis, since lateral load is not taken into consideration in an alternate path (AP) analysis ([7]) (i.e. dead load + 0.25 live load is applied according to GSA guideline). This will under predict the building response compared to the real response of the building frame under a blast. Numerical results for vertical deflection due to columns loss are summarised in Fig. 23a. Deformed view of building frame due to five columns loss is shown in Fig. 16c. It is known that a simple braced frame may be susceptible to progressive collapse for a single column loss (AP) due to weak column-to-beam joint (Jeyarajan et al. [49]). Three and five column loss, causing larger deflection in addition to large end rotation and significant force demand on members and thus frame under 500 kg TNT explosion, is susceptible to progressive collapse. The 10-storey centre core braced simple frame is subjected to partial collapse due to a surface blast load of 500 kg TNT.

Table 5. Maximum demand for frame with 5% damping and without strain rate effect

(a)

Point	Max. lateral deflection (mm) (Z-direction)	Max. minor axis bending moment (kNm)	Max. axial force (kN)	Max. shear force (minor) (kN)	Max. plastic strain
a	−396	513*	4283	345	0.039
b	−288	513*	3309	335	0.035
c	−242	513*	2733	136	0.026
d	−91.2	510	1296	146	0.002
e	−108	453	3949	264	0.003
f	−62.6	385	3039	286	0
g	−88.7	249	2564	196	0
h	−52.9	271	1181	223	0
i	−176	513*	2808	285	0.022
j	−42.8	349	2609	249	0
b_1	−4.78	72.9	823	188	0

* Plastic moment resistance is reached

(b)

Point	Max. lateral deflection (mm) (X-direction)	Max. vertical deflection (mm) (Y-direction)	Max. major axis bending moment (kNm)	Max. torsional moment (kNm)	Max. major axis shear force (kN)
a	127	−37.9	175	28.2	95.9
b	55.7	−21.2	122	20.4	93.5
c	6.12	−13.1	185	18.1	81.3
d	8.76	−2.22	212	20.9	78.6
e	11.4	−56.7	163	22.0	141
f	10.8	−36.1	191	14.8	81.4
g	10.2	−18.4	143	13.8	139
h	6.42	−3.82	191	15.4	108
i	14.1	−7.46	150	10.2	51.1
j	4.14	−11.8	183	11.1	55.2
b_1	5.08	−65.9	972	2.38	122

5. CONCLUSIONS

A simplified composite slab model in which the profile metal deck is represented by rows of rebars and the profile concrete is converted into an equivalent uniform concrete section has been proposed to analyse the collapse behaviour of three-dimensional composite building. Semi-rigid composite joints in the building framework are modelled using the Eurocode's component model represented by linear and rotation spring connectors. The connectors' behaviour is represented by an axial force-displacement relationship and moment-rotation relationship. The proposed slab and joint models, which are validated against experimental results, avoid the detailed finite element modelling of the metal deck profile and joint components and thus improve the efficiency of analysing large building framework subject to accidental load. The proposed models also provide a more realistic estimate of 3-D frame behaviour compared to other frame models assuming pin or rigid joint behaviour.

The beams and columns are modelled using the beam elements rather than shell elements to further improve the computational efficiency of analysing large building framework. Once the maximum resistance of the beam or column is exceeded, it is treated as damaged and removed in the subsequent collapse analysis. The residual resistance of the damaged member is ignored and this will lead to conservative estimate of the progressive collapse resistance of the structure. The proposed simplified models have been verified against the established test and numerical data available in the literature and found to be accurate enough for progressive collapse analysis.

A ten-storey centred core braced simple frame is investigated for a surface blast, which is detonated at a distance away from the front surface of the building. Material strain rate effect due to dynamic blast loading has significant influence on the responses of the composite building. The vertical and lateral deflections of the frame considering strain rate effect are less than those predicted without strain rate effect. The force demands on the frame considering strain rate effect is higher than those without considering the strain rate effect. The increase in dynamic strength and stiffness of materials caused by high strain rate would induce higher forces acting on the member as the structure deforms less. Nonlinear dynamic analysis shows that high blast load may wipe out several columns at the ground floor and induce high shear force on the first storey columns. High blast pressure also caused large lateral drift and significant axial force on the ground floor columns. The study concludes that scenario-base nonlinear dynamic analyses should be performed to capture the true behaviour of buildings subject to high blast load. This approach is more sensible than the alternate path approach checking the robustness of buildings based on the column removal concept. The alternate path approach can be used in preliminary design to check robustness of a building, but nonlinear dynamic analysis based on the proposed simplified models is still preferred for threat-scenario analyses.

ACKNOWLEDGEMENT

The first author wishes to acknowledge the research scholarship make available by the National University of Singapore for his PhD research study in Singapore.

REFERENCES

[1] Izzuddin B.A, Vlassis A.G, Elghazouli A.Y and Nethercot D.A. Progressive collapse of multi-storey buildings due to sudden column loss – Part I: Simplified assessment framework. *Engineering Structures* 2008; 30(5): 1308–1318.

[2] Sadek F, EI-Tawil S and Lew H.S. Robustness of Composite Floor Systems with Shear Connections. *Journal of Structural Engineering* 2008; 134(11): 1717–1725.

[3] Alashker Y, El-Tawil S and Sadek F. Progressive collapse resistance of steel-concrete composite floors. *Journal of Structural Engineering* 2010; 136(10): 1187–1196.

[4] Fu F. 3-D nonlinear dynamic progressive collapse analysis of multi-storey steel composite frame buildings - Parametric study. *Engineering Structures* 2010; 32(12): 3974–3980.

[5] Kwasniewski L. Nonlinear dynamic simulations of progressive collapse for a multistory building. *Engineering Structures* 2010; 32(5): 1223–1235.

[6] Alashker Y, Li H and El-Tawil S. Approximations in Progressive Collapse Modeling. *Journal of Structural Engineering* 2011; 137(9): 914–924.

[7] GSA. GSA Guidelines for Progressive Collapse Anlaysis. U.S. General Services Administration, USA, 2003.

[8] TM-5-1300. Structures to Resist the Effects of Accidental Explosions. TM-5-1300, Departments of the Army, The Navy, The Air force, USA, 1990.

[9] EN1991-1-7. Eurocode 1 – Actions on structures. Part 1-7 General actions- Accidental actions, European Committe for Standardization, 2006.

[10] Shi Y, Li Z.X and Hao H. A new method for progressive collapse analysis of RC frames under blast loading. *Engineering Structures* 2010; 32(6): 1691–1703.

[11] Ngo T, Mendis P, Gupta A and Ramsay J. Blast Loading and Blast Effects on Structures. *eJSE International* 2007; Special Issue-Loading on Structures: 76–91.

[12] Draganic H and Sigmund V. Blast Loading on Structures. *Tehnički vjesnik* 2012; 19(3): 643–652.

[13] Raparla H.B and Kumar R.P. Linear Analysis of Reinforced Concrete Buildings Subjected to Blast Loads. *ICI Journal* 2011; 2011(April–June): 1–16.

[14] Serdar A, Krauthammer T, Morency D and Tran P.T. Behavior of reinforced concrete columns under combined effects of axial and blast-induced transverse loads. *Engineering Structures* 2013; 55(2013): 26–34.

[15] Ganesh T, Kadambi V.A, Robert S and Johnson F.C. Experimental and finite element analysis of doubly reinforced concrete slabs subjected to blast loads. *International Journal of Impact Engineering* 2015; 75(2015):162–1173.

[16] Hosseinipoor S.M.A, Gholamrezae R and Akbarian M. Study of Explosive Resistance Scaling on Reinforced Concrete Slab under Loading, under Free-Air Burst Blast *Indian J.Sci.Res* 2014; 2(2014): 650–659.

[17] Lin X, Zhang Y.X and Hazell J.P. Modelling the response of reinforced concrete panels under blast loading. *Materials & Design* 2014; 56(2014): 620–628.

[18] Zhang D, Yao S.J, Lu F, Chen X.G, Lin G, Wang W and Lin Y. Experimental study on scaling of RC beams under close-in blast loading. *Engineering Failure Analysis* 2013; 33(2013): 497–504.

[19] Said E and Bilal E.A. Progressive collapse evaluation of externally mitigated reinforced concrete beams. *Engineering Failure Analysis* 2014; 40(2014): 33–47.

[20] Li B, Rong H.C and Pan T.C. Drift-controlled design of reinforced concrete frame structures under distant blast conditions - Part II: Implementation and evaluation. *International Journal of Impact Engineering* 2007; 34(4): 755–770.

[21] Li B, Rong H.C and Pan T.C. Drift-controlled design of reinforced concrete frame structures under distant blast conditions – Part I: Theoretical basis. *International Journal of Impact Engineering* 2007; 34(4): 743–754.

[22] Tarek H.A, Elsanadedy H.M, Abbas H, Ngo T and Mendis P. Numerical Analysis for Progressive Collapse Potential of a Typical Framed Concrete Building. *International Journal of Civil & Environmental Engineering* 2010; 10(2).

[23] Jayasooriya R, Thambiratnam P.D and Perera J.N and Kosse V. Blast and residual capacity analysis of reinforced concrete framed buildings. *Engineering Structures* 2011; 33(12): 3483–3495.

[24] Luccioni B.M, Ambrosini R.D and Danesi R.F. Analysis of building collapse under blast loads. *Engineering Structures* 2004; 26(1): 63–71.

[25] Osama A.M. Assessment of progressive collapse potential in corner floor panels of reinforced concrete buildings. *Engineering Structures* 2009; 31(3): 749–757.

[26] Elsanadedy H.M, Almusallam T.H, Alharbi Y.R, Al-Salloum Y.A and Abbas H. Progressive collapse potential of a typical steel building due to blast attacks. *Journal of Constructional Steel Research* 2014; 101(2014): 143–157.

[27] Zolghadr-Jahromi H, Vlassis A.G and Izzuddin B.A. Modelling approaches for robustness assessment of multi-storey steel-composite buildings. *Engineering Structures* 2013; 51(2013): 278–294.

[28] EN1993-1-1. Eurocode 3: Design of steel strcutures. Part 1–1: General rules and rules for buildings, European Committe for Standardization, 2005.

[29] Simulia, ABAQUS documentation 6.11, 2011.

[30] EN1993-1-8. Eurocode 3: Design of steel structures. Part 1–8: Design of joints, European Committe for Standardization, 2005.

[31] EN1994-1-1. Eurocode 4: Design of composite steel and concrete structures. Part 1–1: Genaral rules and rules for buildings, European Committe for Standardization, 2004.

[32] da Silva J.G.S, de Lima L.R.O, da S. Vellasco P.C.G, de Andrade S.A.L and de Castro R.A. Nonlinear dynamic analysis of steel portal frames with semi-rigid connections. *Engineering Structures* 2008; 30(9): 2566–2579.

[33] Anderson D and Najafi A.A. Performance of composite connections: Major axis end plate joints. *J. Construct. Steel Research* 1994; 31(1994): 31–57.

[34] Dasison J.B, Kirby P.A and Nethercot D.A. Rotational stiffness characteristics of steel beam to column connections. *J. Construct. Steel Research* 1987; 8(1987): 17–54.

[35] Liew J.Y.R, Teo T.H and Shanmugam N.E. Composite joints subject to reversal of loading- Part 1: Experimental study. *Journal of Constructional Steel Research* 2004; 60(2004): 221–246.

[36] Romero E.R. Finite element simulation of a bolted steel joint in fire using Abaqus program. Tampere University of Technology, Tampere University of Technology, 2010.

[37] Hu Y, Davison B, Burgess T and Plank R. Component modelling of flexible end-plate coneection in fire. *Steel Structures* 2009; 9(1–15).

[38] FEMA-355D. State of the art report on connection performance. Federal Emergency Management Agency, 2000, pp. 305.

[39] Sarraj M, Burgess I.W, Davison J.B and Plank R.J. Finite element modelling of fin plate steel connections in Fire. University of Sheffield, UK, 2007.

[40] Easterling W.S and Abdullah R. New evaluation and modeling procedure for horizontal shear bond in composite slabs. *Journal of Constructional Steel Research* 2009; 65(4): 891–899.

[41] EN1992-1-1. Eurocode 2: Design of concrete structures. Part 1–1: General rules and rules for buildings, European Committe for Standardization, 2004.

[42] Cornelissen H.A.W, Hordijk D.A and Reinhardt H.W. Experimental determination of crack softening characteristics of normal weight and light weight concrete. *HERON* 1986; 31(2): 45–56.

[43] Abdullah R, Paton-Cole V.P and Easterling W.S. Quasi static analysis of composite slab. *Malaysian Journal of Civil Engineering* 2007; 19(2): 91–103.

[44] Ranzi G, Bradford M.A, Ansourian P, Filonov A, Rasmussen K.J.R, Hogan T.J and Uy B. Full-scale tests on composite steel–concrete beams with steel trapezoidal decking. *Journal of Constructional Steel Research* 2009; 65(7): 1490–1506.

[45] UFC. Design of buildings to resist progressive collapse. USA, Department of Defence, USA, 2009.

[46] SCI, Structural robustness of steel framed buildings, The Steel Construction Institute, UK, 2011.

[47] Fu F. Dynamic response and robustness of tall buildings under blast loading. *Journal of Constructional Steel Research* 2013; 80(2013): 299–307.

[48] SCI, Protection of buildings against explosions, The Steel Construction Institute, 1999.

[49] Jeyarajan S., Liew J.Y.R. and Koh C.G. Progressive collapse mitigation approaches for steel concrete composite buildings. International Journal of Steel Structures, 2015, 15(1), 175–191.

[50] Jeyarajan S., Liew J. Y. R. and Koh C. G. (2015). Enhancing the robustness of steel-concrete composite buildings under column loss scenarios, International Journal of Protective Structures, 6 (3), 529-550.

[51] Jeyarajan S. (2015). Robustness analysis and design of steel-concrete composite buildings. *PhD Thesis, National University of Singapore*.